J Therm Anal Calorim (2010) 99:197–202
DOI 10.1007/s10973-009-0132-2

Thermal analysis of CsH_2PO_4 nanoparticles using surfactants CTAB and F-68

S. Hosseini · A. B. Mohamad · A. H. Kadhum · W. R. Wan Daud

Received: 2 January 2009 / Accepted: 24 March 2009 / Published online: 19 June 2009

Abstract A study concerned to thermogravimetric analysis is performed in cesium dihydrogen phosphate (CsH_2PO_4) that was synthesized, using cetyltrimethylammonium-bromide (CTAB), polyoxyethylene-polyoxypropylene (F-68) and mixture of (F-68:CTAB) with two mole ratio 0.06 and 0.12 as surfactant. The dehydration behavior of particles was studied using thermal gravimetric analysis and differential scanning calorimetric. Subsequently, the experimental results indicated that the first dehydration temperature in the range of 237–239 °C upon heating, the second peaks occur at temperature range 290–295 °C and overlapping in the thermogravimetric events is observed. The mass loss values are obtained in the range of 6.62–6.97 wt% that is less than reported theoretical value 7.8 wt%. These values show well compatibility of reaction CsH_2PO_4 to $Cs_2H_2P_2O_7$ with 3.92 wt% whereas mass loss value of CsH_2PO_4 to $CsPO_3$ is less than theoretical value 7.8 wt%. The activation energy of two steps dehydration are calculated using Kissinger equation for the samples synthesized via CTAB and (F-68) with minimum value mass loss 6.62% and maximum value mass loss 6.97%, respectively. The calculation results reveal that the reaction rate in the first step ($CsH_2PO_4 \rightarrow Cs_2H_2P_2O_7$) is faster than the second step ($CsH_2PO_4 \rightarrow CsPO_3$). The weight loss values of the samples demonstrate that existence of CTAB can be considered as effective factor which prevents more weight loss during the dehydration process.

S. Hosseini (✉) · A. B. Mohamad · A. H. Kadhum · W. R. Wan Daud
Institute of Fuel Cell, University Kebangsaan Malaysia, 43600 Bangi, Selangor, Malaysia
e-mail: hosse_so@yahoo.com

Keywords CsH_2PO_4 · Dehydration · Nanoparticle · Surfactants

Introduction

Solid acids follow chemical composition such as $M_aH_b(XO_4)_c$, where (M = K, Rb, Cs, NH_4; X = S, Se, P) and a, b, c are their respective stoichiometric coefficients [1]. Cesium dihydrogen phosphate (CsH_2PO_4) is a member of the solid acid family that is built from the discrete PO_4 tetrahedral connection of O–H···O hydrogen bonds and through the electrostatic interaction of the cesium cation. Moreover, solid acids show high proton conductivity in the superprotonic phase 230 °C along with the breakage of hydrogen bonds and the rotational motion of the XO_4 tetrahedrons. CsH_2PO_4 (CDP) crystal undergoes three phase transitions that the first phase is ferroelectric starting at $T_c = 153$ K (monoclinic), upon to increase temperature, the second is paraelectric at room temperature [2, 3]. This phase is recognizable by a monoclinic structure with the space group $P2_1/m$ and two formula units per cell ($Z = 2$), which are characterized by the disorder of the acid proton on the hydrogen bond network, that link the tetrahedral group PO_4 [4]. The third phase, the superprotonic phase transition, is distinguishable by rapid proton transfer and the liberation of oxy-anion at 504 K [5–7].

$$\underset{(\text{monoclinic})}{\text{Ferroelectric}} \rightarrow \underset{(\text{monoclinic})}{\text{Paraelectric}} \rightarrow \underset{\text{Cubic}}{\text{Superprotonic}}$$

The superprotonic transition of CsH_2PO_4 at temperature 230 °C with cubic symmetry taking into account experimental results by DSC [7–11] and thermal expansion [12] in which proton conductivity increases sharply in order of 10^{-3} to 10^{-2} S cm^{-1}. Metcalfe et al. reported CsH_2PO_4

undergoes two transitions at 149 °C and 230 °C in which the lower one is quasi-irreversible with enthalpy of 4.284 kJ mol^{-1} and another at 230 °C is fully reversible with enthalpy of 1.071 kJ mol^{-1} and mass loss of 1.5% [8]. Wada et al. studied high-temperature properties of CsH_2PO_4 single crystals that confirmed only one the transition at 230 °C without any peak at 149 °C [13]. Gupta et al. investigated thermal behaviour of CsH_2PO_4 as a reversible polymorphic phase transition at 235 °C with mass loss have been continued at 415 °C [14]. Baranov et al. show a phase transition at 230 °C that conductivity of proton increases two to three orders of magnitude, reaching values as high as 10^{-2} Ω^{-1} cm^{-1} [15]. Boysen et al. resulted an enthalpy 49 ± 2.5 J g^{-1} at 228 ± 2 °C just prior to thermal decomposition that highly depend on sample surface area whereas the structural transformation (superprotonic) was not depend on to surface area [6]. The high proton conductivity, at temperature 230 °C can be utilized as an anhydrous membrane in intermediate temperatures fuel cell (150–260 °C). The aim of this work is the investigation of CsH_2PO_4 thermal behavior that synthesized using surfactants such as CTAB, F-68, (F-68: CTAB)0.06 and (F-68: CTAB)0.12 with different morphology.

Experimental

CsH_2PO_4 was prepared using surfactants such as CTAB, F-68, (F-68:CTAB)0.06 and (F-68:CTAB)0.012. Stoichiometric amounts of high purity starting reagents Cs_2CO_3, H_3PO_4 and deionized water were mixed thoroughly with surfactant solutions such as (CTAB + ethanol), (F-68 + ethanol) and (F-68:CTAB + ethanol) separately for 8 h as shown in Fig. 1. The resultant solution was washed several times with acetone to remove the remaining surfactants. The white precipitate is separated by a vacuum pump from the slurry solution. The powder was dried at 130 °C overnight in order to evaporate any water. The calcinations of powders follow heating at constant temperature 220 °C for 8 h, under N_2 gas. Powder X-ray diffraction analysis was performed using a diffractometer (D&Advance) with the following conditions Cu$K\alpha_1$ in the 2Θ range, from 2.3° to 60°. Surface morphologies and particles size were studied using a Scanning Electron Microscope (LEO 1450VP, 20KV) and Transition Electron Microscopy (Philips CM-12, 100KV). Thermogravimetric analyses were performed using thermal gravimetric analysis (SDTA851 METTLER TOLEDO) and differential scanning calorimetric (SDTA822) between 30 °C and 600 °C at heating rate 5 °C min^{-1} under a stream of nitrogen. The samples were heated in alumina pan, at certain heating rate and amount (~20 mg).

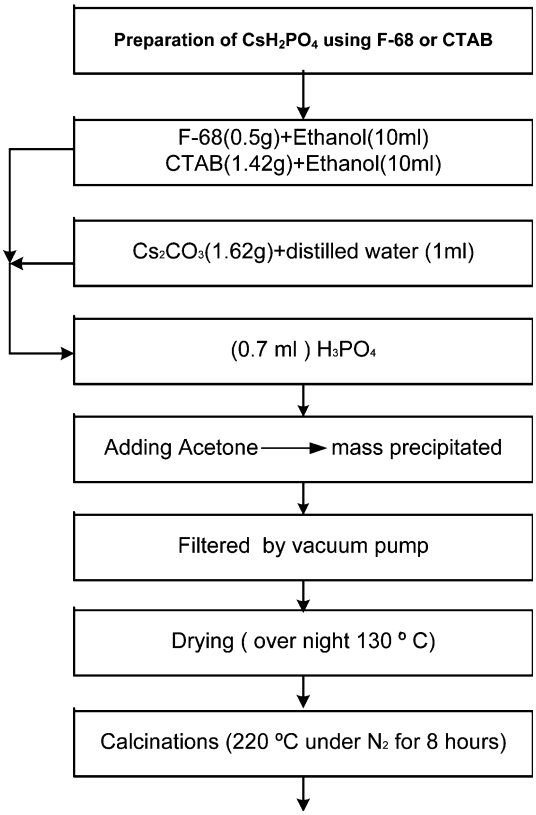

Fig. 1 Scheme of the CDP synthesizes process using CTAB or F-68

Results and discussion

The XRD pattern of the four samples were acquired in range 2.3–60° and all of the diffraction peaks can be readily indexed from the standard powder diffraction file of the monoclinic phase CsH_2PO_4 (JCPDS code No. 084-0122). It can be seen that the samples reveal similar lattice parameters and well coincidence with parameters a = 7.912, b = 6.386, c = 4.88 and β = 107.73. The particles size distribution was determined from transmission electron microscope (TEM) images that are based on an automated image analysis. The normal size distribution of the particles are calculated by mathematical equations or Excel functions, comprising of various parameters such as mean (AVRAGE), standard deviation (STDEV) and normal distribution (NORMDIST) that average size for four samples is listed in Table 1. The surface morphology of samples using SEM show the samples $CDP_{F\text{-}68}$, CDP_{CTAB}, $CDP_{(F\text{-}68:CTAB)0.06}$ and $CDP_{(F\text{-}68:CTAB)0.12}$ exhibit spherical, rod-like, cubic and irregular shape, respectively. The different morphologies may be arisen from the different templates that the surfactants solution made during synthesis such as reveres micelle, cylinders etc. that is depend on to critical micelle concentration (CMC) of surfactants. The thermal properties of samples were studied by the differential scanning calorimetry (DSC) and thermogravimetric

Table 1 Surface morphology and size particles of four samples CDP using surfactants

Sample	Average size (nm)/morphology
$CDP_{F\text{-}68}$	2.66 (spherical)
CDP_{CTAB}	3.7 (rod-like)
$CDP_{(F\text{-}68:CTAB)0.06}$	3.5 (cubic)
$CDP_{(F\text{-}68:CTAB)0.12}$	4.89 (irregular shape)

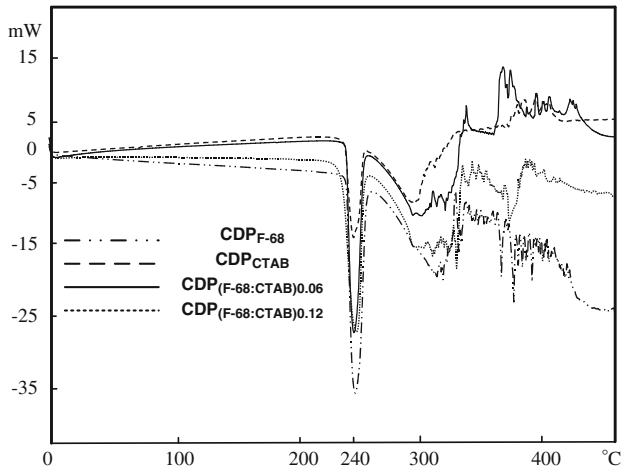

Fig. 2 DSC curves (dehydration peaks) of four samples CsH_2PO_4

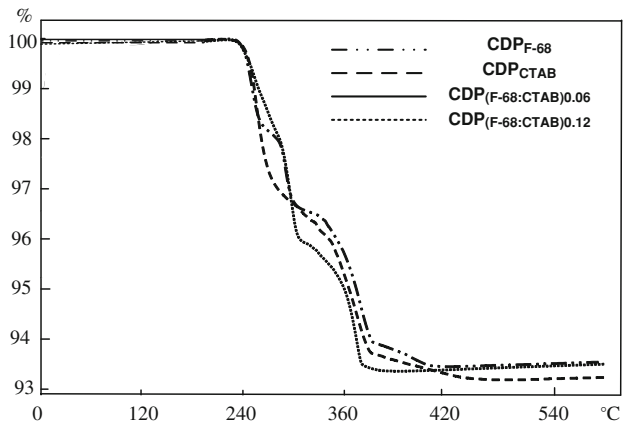

Fig. 3 TG curves (mass loss) of four samples CsH_2PO_4

analysis (TG) simultaneously. Differential Scanning Calorimetry (DSC) measurements, using a heating rate of 5 °C min^{-1}, are performed on four samples of CsH_2PO_4 as shown in Fig. 2. The peaks are observable in the DSC measurements that are consistent to the TG results (%mass loss), as shown in Fig. 3. Figure 2 shows the DSC spectra measured during heating rate of 5 °C min^{-1} for $CDP_{F\text{-}68}$, CDP_{CTAB}, $CDP_{(F\text{-}68:CTAB)0.06}$ and $CDP_{(F\text{-}68:CTAB)0.12}$ samples with noticed peaks more than two step. The peaks at range 233–350 °C can be observed during heating corresponding to mass loss steps in TG analysis. In Fig. 2, the endothermic peak below 250 °C was accompanied by a mass loss around 3 wt%, indicating the dehydration of the crystallized water. This implies that the crystallized water had been lost or possibly displaced by organic molecules that are more thermally stable (CsH_2PO_4). The second endothermic peak shows the transformation of dehydration product to stable product around 300 °C. The endothermic peak of the DSC curve around 380 °C is considered to be the melting process of CsH_2PO_4 in cases CDP_{CTAB}, $CDP_{(F\text{-}68:CTAB)0.06}$ unlike to the other samples. According to the TG curve, the decomposition process took place mainly in the temperature range of 260–350 °C.

The overall dehydration process might consist of two simple processes: the breaking of hydrogen bonding and the rapid escape of water from hydrate. The former is more related with IR spectral change, while the latter is easily obtained by TG. The measured enthalpies and mass loss values are listed in Table 2. The dehydration reaction according to this pathway is described as [16]:

$$CsH_2PO_4 \rightarrow Cs_2H_2P_2O_7 \rightarrow CsPO_3$$

The dehydration of CsH_2PO_4 occurs by two steps, in which the material first forms $CsH_2P_2O_7$ that subsequently dehydrate to $CsPO_3$. The final product $CsPO_3$ is the thermodynamically stable phase even at temperature just above T_{dey} as measured from the conductivity experiments [16], however, $CsH_2P_2O_7$ is a intermediate product that produce under isothermal and constant heating conditions. Uda et al. suggested the reaction rate of the first step (CsH_2PO_4 to $CsH_2P_2O_7$) is faster than the second step (CsH_2PO_4 to $CsPO_3$) that arisen of the structural different between three components including PO_4^-, $P_2O_7^-$ and $CsPO_3$ [17]. The dehydration reactions, followed by thermal processes are suggested as follows [16]:

$$nCsH_2PO_4 \rightarrow Cs_nH_2P_nO_{3n+1} + (n-1)H_2O$$

The two final products are examined by the dehydration reactions of the different values of n in the above reaction. The theoretical calculations of the mass losses are based on the remaining products ($Cs_2H_2P_2O_7$, $CsPO_3$) and the evaporated products (H_2O), as following:

$$CsH_2PO_4 \rightarrow Cs_2H_2P_2O_7 + H_2O \quad (n = 2)$$

Table 2 Weight loss, enthalpy values of four samples of CDP

Sample	Weight loss (wt%)	Enthalpy (J g^{-1})
$CDP_{(F\text{-}68)}$	6.97	51.23 ± 0.6
$CDP_{(CTAB)}$	6.62	49.07 ± 0.5
$CDP_{(F\text{-}68:CTAB)0.06}$	6.71	37.3 ± 0.5
$CDP_{(F\text{-}68:CTAB)0.12}$	6.63	48.06 ± 0.5

$$\frac{Cs_2H_2P_2O_7}{2CsH_2PO_4} \times 100 = 96.08\%,$$
$$\frac{H_2O}{2CsH_2PO_4} \times 100 = 3.92\%$$

$$CsH_2PO_4 \rightarrow CsPO_3 + H_2O \ (n \gg 1)$$

$$\frac{CsPO_3}{CsH_2PO_4} \times 100 = 92.16\%, \quad \frac{H_2O}{2CsH_2PO_4} \times 100 = 3.92\%$$

The reaction of $Cs_2H_2P_2O_7$ to $CsPO_3$ is follows:

$$Cs_2H_2P_2O_7 \rightarrow 2CsPO_3 + H_2O$$

$$\frac{2CsPO_3}{Cs_2H_2P_2O_7} \times 100 = 95.92\%,$$
$$\frac{H_2O}{Cs_2H_2P_2O_7} \times 100 = 4.072\%$$

According to these reactions, the first product resulted via reaction CsH_2PO_4 to $Cs_2H_2P_2O_7$ that has value 3.92% mass loss whereas upon to the increase temperature during process the product change to $CsPO_3$ with 7.8% mass loss. The dehydration process is endothermic during process and it can be analyzed as usual by the onset (T_{onset}), peak (T_{dey}), and endset (T_{endset}), temperatures and heat flow by the area under the peak. In the Fig. 2, the DSC curves of the dehydration show the complete separation of both dehydration processes is not possible. The endset temperature (the temperature at which the event can be considered as finished) for the first dehydration and the onset temperature (the temperature at which the event has begun) for the second dehydration are overlapped. It seems that the apparent activation energies are very close (within the limits of experimental errors) for both steps that can be calculated using Kissinger's method [18].

In the Table 3, different thermogravimetric values are summarized that the onset/endset temperature values for the first dehydration and the endset temperature value for the second dehydration. The dehydration process occurs in multiple steps as shown in Table 3 that all steps reveal in Fig. 2. The samples CDP_{CTAB}, $CDP_{(F\text{-}68:CTAB)0.06}$ and $CDP_{(F\text{-}68:CTAB)0.12}$ are observed only in two step of dehydration, whereas the sample $CDP_{F\text{-}68}$ occurred in one step more (third step) at temperature 350 °C. Quit significantly, regardless of samples (using different surfactant or alcohols), in all cases a phase transition independent of decomposition is evident at 230 ± 1 °C that is determined by conductivity measurement [17].

The enthalpy of dehydration process was calculated by integral of heat flow during process with heating rate 5 °C min^{-1}. The enthalpy values of samples $CDP_{F\text{-}68}$, CDP_{CTAB}, $CDP_{(F\text{-}68:CTAB)0.06}$ and $CDP_{(F\text{-}68:CTAB)0.12}$ are calculated as 51.23 ± 0.6, 49.07 ± 0.5, 37.3 ± 0.5 and 48.064 ± 0.5, respectively. These values has coincidence with Boysen's value 49.0 ± 2.5 J g^{-1} that obtained from a single crystal with heating rate of 5 °C min^{-1}, whereas sample $CDP_{(F\text{-}68:CTAB)0.06}$ has a value less than the other samples and Boysen's value. The mass loss values and the thermal behaviors of four samples is shown in Fig. 3. The minimum and maximum mass loss values are reported in

Table 3 Three steps of dehydration temperatures of four samples CDP

Sample	First			Second (°C)	Third (°C)
	T_{Onset} (°C)	T_{dey} (°C)	T_{Endset} (°C)		
$CDP_{(F\text{-}68)}$	233	237	245	290	347
$CDP_{(CTAB)}$	233	238	244	292	
$CDP_{(F\text{-}68:CTAB)0.06}$	234	237	244	290	
$CDP_{(F\text{-}68:CTAB)0.12}$	233	239	244	293	

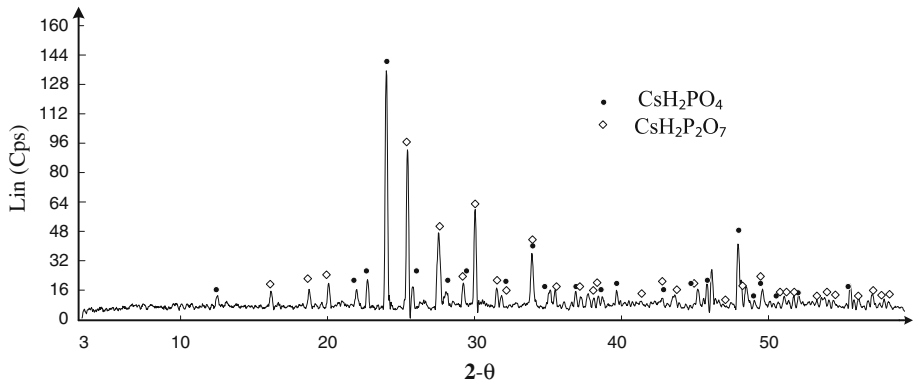

Fig. 4 XRD pattern of resultant dehydration process

range (6.62–6.97) wt% for CDP_{CTAB} and $CDP_{(F\text{-}68)}$, respectively. In three case, $CDP_{(CTAB)}$, $CDP_{(F\text{-}68:CTAB)0.06}$ and $CDP_{(F\text{-}68:CTAB)0.12}$ obtained the values 3.31, 3.08 and 3.92% for the first step of dehydration that show approximately the same theoretical value as mentioned (3.92%) for the first reaction of dehydration whereas $CDP_{(F\text{-}68)}$exhibited a value 1.504% for this step that is not compatible with (3.92%). This difference show existence strong bonds between H_2O and $CDP_{(F\text{-}68)}$ on outer surface in compare to other samples in which more mass loss occur in second stage around 5.48 wt%. The XRD result shows existence CsH_2PO_4 and $Cs_2H_2P_2O_7$ as remaining products in dehydration reaction in JCPDS File Card as shown in Fig. 4 [19]. Haile et al. report that the mass loss of the CDP powder reaches the value of 1.9% (consist of CsH_2PO_4 and $Cs_2H_2P_2O_7$) and 6% (consist to $Cs_2H_2P_2O_7$ and $CsPO_3$) [6]. The results show well agreement with Haile's result.

The activation energy of each dehydration steps was determined using Kissinger's method in which is known as the Kissinger–Akahira–Sunose (KAS) method [20]. The Kissinger equation is given as follows:

$$\mathrm{Ln}\left(\phi/T_{\mathrm{m}}^{2}\right) = \text{constant} - \frac{E_{\mathrm{a}}}{RT_{\mathrm{m}}}$$

Where the heating rate, ϕ (°C min^{-1}) and the temperature at peak maximum, T_m (K) are plotted due to obtain activation energy in Kissinger's equation. This equation is derived with the assumption that the rate of reaction is maximal at the temperature which the endothermic peak reaches a maximum value.

The activation energy can be determined from experiments at various heating rates. Plotting $\ln(/T_m^2)$ versus $1/T_m$ can be calculate E_a for prediction in any step during dehydration. The slope of this equation gives activation energy, regardless of the reaction order of the system. The samples CDP_{CTAB} and $CDP_{(F\text{-}68)}$ are conducted in four heating value 1, 5,10 and 15 °C min^{-1} in order to investigation of activation energy at different steps. The selection of these samples was based on minimum and maximum mass loss values 6.62% and 6.97% with almost the same particles size. The activation energy of two dehydration steps is calculated by Kissinger equation as seen in Table 4. The results show the low values of the activation energy obtained for the first step that is compatible with Uda et al. [17]. The low value in the first step can be considered that dehydration CsH_2PO_4 to $Cs_2H_2P_2O_7$ is faster than formation $CsPO_3$. Generally, the activation energy of dehydration will be affected by both particle size and sample mass. With a larger sample mass and smaller particles due to the increased surface area will promote dehydration and therefore reduce E_a. This could result from the enhanced dehydration due to the greater ratio of surface area/volume of the smaller particles. The particles size of two samples is almost close to together, thus, the surface morphology and the CTAB amount can be affected in dehydration process.

Table 4 Calculation of activation energy using Kissinger method for two steps of CDP_{CTAB} and $CDP_{F\text{-}68}$

Dehydration step	CDP_{CTAB} (kJ mol^{-1})	$CDP_{(F\text{-}68)}$ (kJ mol^{-1})
First step	27.503 ± 0.89	27.377 ± 1.03
Second step	34.34 ± 2.15	35.04 ± 1.98

Conclusion

The synthesis of the CsH_2PO_4 nanoparticles is achievable by adding the limpid solutions as CTAB, F-68 and the mixture (F-68:CTAB) to aqueous solution (Cs_2CO_3, H_3PO_4). The particles size measurement show average particles size less than 7 nm with the different surface morphology. According to the results of the experiment, the dehydration temperature of all samples is started at 233 °C with two dehydration steps except $CDP_{(F\text{-}68)}$ has three stage because the smallest particles size more surface area. The activation energy calculation using Kissinger method show the first step of dehydration (CsH_2PO_4 to $Cs_2H_2P_2O_7$) is faster than the second step (CsH_2PO_4 to $CsPO_3$). The maximum value 6.92% and minimum value 6.62% of mass losses are obtained for samples with the average particles size are almost 3.5 nm, thus the surfactants can be effective in process. The comparison of four samples reveal that CTAB can be accounted as preventable factor on more mass loss during the thermal behaviors.

Acknowledgements The authors appreciate the financial support of the IRPA-02-02-02-0006 PR0023/11-08. This work was conducted at the Institute of Fuel Cell University Kebangsaan Malaysia, Selangor, Malaysia.

References

1. Haile SM, Chisholm CRI, Boysen DA, Sasaki K, Uda T. Solid acid proton conductors: from laboratorycuriosities to fuel cell electrolytes. Farad Disc. 2007;134:17–39.
2. Baranov AI, Grebenev W, Khodan AN, Dolbinina VV, Efremova EP. Optimization of superprotonic acid salts for fuel cell applications. Solid State Ionics. 2005;176:2871–4.
3. Otomo J, Minagawa N, Wen C, Eguchi K, Takahashi H. Protonic conduction of CsH_2PO_4 and its composite with silica in dry and humid atmospheres. Solid State Ionics. 2003;156:357–69.
4. Haile SM. Materials for fuel cells. Mate Today. 2003;18:24–9.
5. Baranova AI, Kopnin EM, Grebenev VV, Sin A, Zaopo A, Dubitsky Y, et al. Influence of humidity and thermal decomposition on the protonic conductivity of single and polycrystalline CsH_2PO_4. Solid State Ionics. 2007;178:657–60.
6. Boysen DA, Hiale SM, Liu H, Secco RA. High-temperature behavior of CsH_2PO_4 under both ambient and high pressure conditions. Chem Mater. 2003;15:727–36.

7. Bronowska W. Does the structural superionic phase transition at 231 1C in CsH_2PO_4 really not exist? J Chem Phys. 2001;114:611–2.
8. Metcalfe B, Clark JB. Differential scanning calorimetry of RbH_2PO_4 and CsH_2PO_4. Thermochim Acta. 1978;24:149–53.
9. Kucheyev SO, Bostedt C, Van Buuren T, Willey TM, Land TA, Terminello LJ, et al. Electronic structure of $KD_{2x}H_{2\ (1-x)}\ PO_4$ studied by soft x-ray absorption and emission spectroscopies. Phys Rev B. 2004;B70:245106–12.
10. Lee KS. Hidden nature of the high-temperature phase transitions in crystals of KH_2PO_4-type: is it a physical change? J Phys Chem Solids. 1996;57:333–42.
11. Bronowska W, Pietraszko A. X-ray study of the high-temperature phase-transition of CsH_2PO_4 crystals. Solid State Commun. 1990;76:293–8.
12. Rajendran S, Mahendran O. Experimental investigations on plasticized PMMA/PVA polymer blend electrolytes. Inetr J Ionic. 2001;7:463–9.
13. Wada M, Sawada A, Ishibashi Y. Some high-temperature properties and the Raman-scattering spectra of CsH_2PO_4. J Phys Soc Japan. 1979;47:1571–4.
14. Gupta LC, Rao URK, Venkateswarlu KS, Wani BR. Thermal stability of CsH_2PO_4. Thermochimica Acta. 1980;42:85-90.
15. Baranov AI, Khiznichenko VP, Sandler VA, Shuvalov LA. Frequency dielectric dispersion in the ferroelectric and superionic phases of CsH_2PO_4. Ferroelectrics. 1988;81:1147–50.
16. Park JH. Possible origin of the proton conduction mechanism of CsH_2PO_4 crystals at high temperatures. Phys Rev. 2004;B69: 054104–6.
17. Uda T, Taninaouchi YK, Awakura Y, Ikeda A, Haile SM. Dehydration behavior of the suerorotonic conductor CsH_2PO_4 at moderate temperature: 230 to 260 ^oC. Electrochem J Mater Chem. 2007;17:3182–9.
18. Burnham AK, Weese RK, Wemhoff AP, Maienschein JL. A historical and current perspective on predicting thermal behavior. J Therm Anal Calorim. 2007;89:407–11.
19. JCPDS-ICDD 1995;35:746.
20. Sánchez-Jiménez PE, Criado JM, Pérez-Maqueda LA. Kissinger kinetic analysis of data obtained under different heating schedules. J Therm Anal Calorim. 2008;94:427–32.